INTERACTIVE POLYGONS IN REGION-BASED DEFORMABLE CONTOURS FOR MEDICAL IMAGES

Yaoyao Zhu, Tian Shen, Daniel Lopresti, Xiaolei Huang

Department of Computer Science and Engineering
Lehigh University
Bethlehem, PA 18015

ABSTRACT

A new user interaction method called interactive polygons is presented in this paper. These interaction polygons are designed for use with the Active Volume Model segmentation method [1], which deforms with constraints from both Region Of Interest (ROI) and image gradient information. The two kinds of interaction polygons we apply are "merge polygons" and "split polygons" which identify the foreground and background, respectively. Users are allowed to draw these polygons to correct the original AVM segmentation results. These interactive polygons are used to update the region statistics in the original model and help the model deform to the desirable boundaries.

Index Terms— Segmentation, interactive segmentation, user interaction, active volume models, snakes

1. INTRODUCTION

Boundary extraction is an important task in medical image analysis. The main challenge is to retrieve high-level information from low-level image signals while minimizing the effect of noise, intensity inhomogeneity, and other factors. Model-based methods have been widely used with considerable success. We have proposed a novel deformation-based method, called Active Volume Model (AVM)[1] which deforms with constraints from both Region Of Interest (ROI) and image gradient information. The ROI, which represents the predicted object, is obtained from a classification of image features based on model-interior statistics. An approximation of the object appearance statistics, the model-interior statistics are learned adaptively during model evolution. An advantage of the AVM model is that its formulation allows the ROI information to naturally become part of the Snake's external forces; in this way, rapid model deformations can be derived by finding the solution of the Euler equations in a variational framework [2]. Experiments show that the AVM model performs better for most medical images than other gradient-based active contour models in robustness and accuracy.

For some medical images, however, for example those with complex objects in cluttered backgrounds, the AVM model may fail due to similar appearance between the foreground and some background objects. In these cases, user interaction can help. For snake-like deformable models, the traditional user interactive controls are so-called soft points and hard points [3]. Soft points are attraction points which can incorporate the external forces into the model. Hard points are the points through which the segmentation contour is forced to pass. Some deformable models [4] even allow users to pull the controllable points to the correct positions. Although these interaction methods are convenient, the interaction could be very tedious, for example, users may need to add many attraction points to make the segmentation curve deform to the right edges. Adding hard points or moving the control points could make the segmentation contours no longer smooth.

As for user interaction in our AVM method, we can take advantage of the fact that AVM integrates the model-interior statistics and deforms with constraints from ROI. In this paper, we explore a new user interactive method which is similar to the scribbles used in other interactive segmentation methods such as the random walker method [5] and many MRF based methods [6]. Users can draw polygons in the background or the foreground in addition to the original deforming contour. These polygons are called "merge polygons" if they are drawn in the foreground, and "split polygons" if drawn in the background. From these polygons, we calculate the statistic information for ROI region or background region. Then we incorporate these information into the original deformable model. Thus, the performance of the deformable model can be improved. The process can be iterated until the desired contour is obtained.

We demonstrate that our interactive polygons can be very helpful in segmenting imhomogeneous images. Although there are some algorithms [7] which can automatically segment such images, these algorithms still have parameters which must be manually adjusted to get good results. These parameters are not very intuitive to users who are unfamiliar with segmentation methods, while our interactive polygons can be easily understood and manipulated until the desired segmentations are achieved.

2. ACTIVE VOLUME MODEL

An active volume model is a deforming solid that minimizes internal and external energy. The internal constraint ensures the model has a smooth boundary. The external constraints come from image data, priors, and/or user-defined features. Representing the model boundary parametrically, $\mathbf{v}(s) = (x(s), y(s))$, the internal energy term of AVM is defined similar to Active Contour Models.

$$E_{int} = \int_0^1 (\alpha(s)|\mathbf{v}_s(s)|^2 + \beta(s)|\mathbf{v}_{ss}(s)|^2)ds \quad (1)$$

The external energy function consists of two terms: the gradient term E_g and the region term E_R. So the overall energy function is:

$$E = E_{int} + E_{ext} = E_{int} + k \cdot (E_g + k_{ext} \cdot E_R) \quad (2)$$

where k is a constant that balances the internal and external forces. k_{ext} is a constant that balances the contributions of the gradient term and the region term.

The gradient data term can be defined using the gradient map, edge distance map, or a combination of both. The region data term is a novel aspect of the active volume model, in which it learns the appearance statistics of the object of interest dynamically and the model's deformation is driven by the predicted object-region boundary. This is also the focus of our new interaction method.

Let us consider that each constraint corresponds to a probabilistic boundary prediction module and suppose we have n independent external constraints, the feature used in the kth constraint is f_k, and $L(\mathbf{v})$ denotes the label of a pixel $\mathbf{v}$, our approach to combining the multiple independent modules involves the Bayes rule in order to evaluate the final confidence rate:

$$\begin{aligned} Pr(L(\mathbf{v})|f_1, ..., f_n) &= \frac{Pr(f_1, ..., f_n|L(\mathbf{v}))Pr(L(\mathbf{v}))}{Pr(f_1, ..., f_n)} \\ &\propto Pr(f_1|L(\mathbf{v}))...Pr(f_n|L(\mathbf{v}))Pr(L(\mathbf{v})) \end{aligned} \quad (3)$$

For each independent module, the probability $Pr(f_k|L(\mathbf{v}))$ is estimated based on the active volume model's interior statistics. Considering a module using intensity statistics, the object region can be predicted according to the current model-interior intensity distribution. For instance, for a pixel $\mathbf{v}$ with intensity feature value $I(\mathbf{v}) = i$ where i ranges from 0 to 255, we have:

$$\begin{aligned} Pr(i|I) &= Pr(i, obj|I) + Pr(i, non\_obj|I) \\ &= Pr(i|obj, I)Pr(obj|I) \\ &+ Pr(i|non\_obj, I)Pr(non\_obj|I) \end{aligned} \quad (4)$$

In the equation, the intensity distribution over the entire image I, $Pr(i|I)$, is known, and we estimate the object-interior distribution $Pr(i|obj, I)$ by the current model-interior intensity distribution. Therefore, the background distribution can be derived:

$$Pr(i|non\_obj, I) = \frac{Pr(i|I) - Pr(i|obj, I)Pr(obj|I)}{Pr(non\_obj|I)} \quad (5)$$

Assuming a uniform prior, $Pr(obj|I) = Pr(L(\mathbf{v}) = obj) = 0.5$ and $Pr(non\_obj|I) = Pr(L(\mathbf{v}) = non\_obj) = 0.5$, in Eqn. 5, we are able to compute the background probability $Pr(i|non\_obj, I)$. Applying the Bayesian Decision rule, we can obtain a binary map P_B that represents the predicted object region; that is, $P_B(\mathbf{v}) = 1$ if $Pr(i|obj, I) \geq Pr(i|non\_obj, I)$, and $P_B(\mathbf{v}) = 0$ otherwise. We then apply a connected component analysis algorithm on P_B to retrieve the connected component that overlaps the current model. This connected region is considered as the current ROI. Let us denote the signed distance transform of the current model's shape as Φ_M, and the signed distance transform of the ROI shape as Φ_R, the region-based external energy term is:

$$E_R = \int_0^1 \Phi_M(\mathbf{v}(s))\Phi_R(\mathbf{v}(s))ds \quad (6)$$

The multiplicative term provides two-way balloon forces that deform the model toward the predicted ROI boundary.

3. MOTIVATION FOR EMPLOYING USER INTERACTION

In this section, we discuss some failure cases using AVM and give an analysis as to why AVM fails. Fig. 1 shows a synthetic example for which AVM fails. As can be seen, the left part of the polygon is missing in the projected ROI. In the current

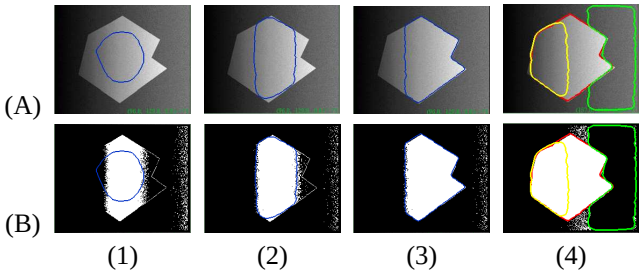

Fig. 1. Synthetic example segmentation using AVM. (A) The model on the original image. (B) The binary map P_B estimated by intensity-based likelihood maps and applying the Bayesian Decision rule. (1) Initial model. (2) The model after 12 iterations. (3) Final result after 26 iterations without interactive polygons ($p = 0.74$, $q = 0.97$). (4) Final result with interactive polygons (merge polygon in yellow and split polygon in green) ($p = 0.99$, $q = 0.98$). (Note: all figures in the paper are best viewed in color)

AVM, we only calculate the intensity distribution of the foreground and background and use them to obtain a ROI binary map. The idea works fine for most medical images where the

assumption that the intensity is homogeneous within the object holds. For certain non-homogeneous images, AVM may be confused when pixels with a certain intensity in one area of the image belong to the foreground while other pixels with the same intensity belong to the background in a different part of the image. Using the image in Fig. 2 as an example, pixels in the area A have the same intensity as pixels in the area B while they belong to the foreground and the background, respectively. We plot the intensity distribution of the foreground and the background in Fig. 2(b). As can be seen, the distribution of the background shown in the blue box dominates the distribution of the foreground, thus we treat pixels with intensity values in the blue box as the background ones and the left portion of the polygon is mistakenly marked as the background in the ROI binary map. The segmentation contour could not deform to the left part of the polygon because of the external forces coming from the region term.

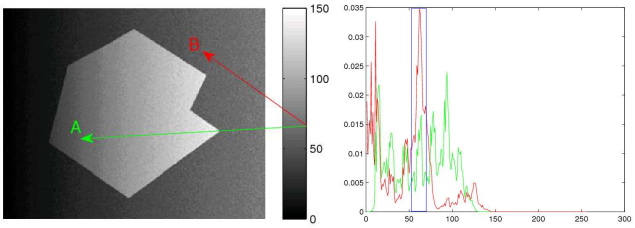

(a) (b)

Fig. 2. Synthetic example (a) The intensity overlap. (b) The intensity distribution of the foreground (green) and the background (red).

Similar situations arise in some medical images. One example is magnetic resonance (MR) images, which exhibit intensity inhomogeneity due to the bias field. The bias can cause serious misclassification when intensity-based segmentation algorithms are used. Essentially, the misclassification is due to an overlap of the intensity ranges of different tissues introduced by the bias field, so that voxels in different tissues are not separable based on their intensities. Intensity inhomogeneities also often occur in images of other modalities, such as X-ray and computed tomography images [7]. Fig. 3 shows a failure case in a spine image where the part in the red circle is mistakenly left out.

4. INTEGRATING USER INTERACTION TO AVM

The analysis in the previous section suggests that intensity information itself is not sufficient for segmentation of inhomogeneous images. User interaction can help in these cases since human eyes are normally good at distinguishing the background and the foreground with high reliability. The interaction we introduce here are polygons that the user draws in the background or in the foreground to help the active contour deform to the desired boundary. The polygons in the background, i.e., split polygons, are there to prevent the active contour from leaking to the background. The polygons

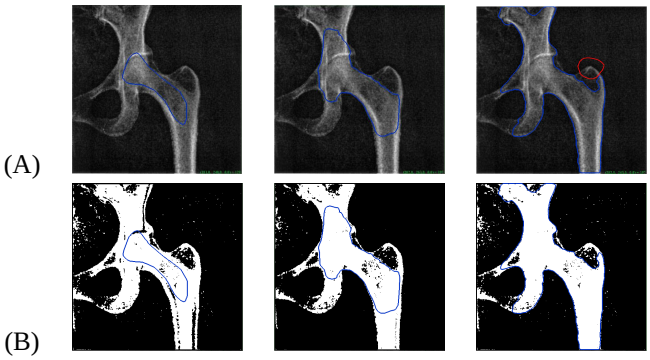

Fig. 3. X-ray spine image segmentation using AVM. (A) The model on the original image. (B) The binary map P_B estimated by intensity-based likelihood maps and applying the Bayesian Decision rule. (1) Initial model. (2) The model after 23 iterations. (3) Final result after 84 iterations.

in the foreground, i.e., merge polygons, are there to help the active contour flow into the foreground.

With merge/split polygons, we cannot assume uniform priors anymore in Eqn. 5. Instead, we calculate the priors for each pixel according to its distances to the merge or split polygons. We use the following notations to describe how to calculate binary ROI map P_B using the priors of $Pr(obj|I)$, $Pr(non\_obj|I)$.

1. Let $s(n,m)$ be a pixel on image Ω. s's position is $(n,m), n = 1,...,N, m = 1,...,M$. s's intensity is $i = I(n,m)$;
2. $P_k, k = 1,...,K$: K merge polygons drawn by users including the original deformable contour which is viewed as foreground;
3. $Q_l, l = 1,...,L$: L split polygons drawn by users;
4. $P_B(n,m)$: binary ROI image;

We incorporate the spatial information into the distribution function by adding priors which are functions of the distance to interactive polygons. The original contour and interactive polygons can deform in parallel or separately by users' choices. In our interactive model, merge/split polygons can also be deformed using AVM. The region statistics of the original contour are incorporated in a similar way since we treat the original contour as a special case of a merge polygon. If a pixel is in a merge or split polygon, then the corresponding pixel in the ROI binary map is set to 255 or 0 respectively. Otherwise, if the intensity value of a background pixel in the original contour appears in both the background and foreground (for instance, pixels in the blue box in Fig. 2(b)) we then calculate its priors according to its distances to the split polygon and the merge polygon, if they exist, as shown in Eqn. 7.

$$\begin{aligned} Pr(obj|I) &= \frac{d(s,P)^{-1}}{d(s,P)^{-1} + d(s,Q)^{-1}} \\ Pr(non\_obj|I) &= \frac{d(s,Q)^{-1}}{d(s,P)^{-1} + d(s,Q)^{-1}} \end{aligned} \tag{7}$$

Where $d(s, P_k)$ is defined as the distance between pixel s and polygon P_k, so $d(s, P) = \min_k d(s, P_k)$ and $d(s, Q) = \min_l d(s, Q_l)$.

Then we use Eqn. 5 to calculate $Pr(i|non\_obj, I)$. Alg.1. summarizes our algorithm.

Algorithm 1 Calculate binary ROI map P_B

for n = 1 to N **do**
  for m = 1 to M **do**
    if $s(n, m)$ inside any $P_k, k = 1, ..., K$ **then**
      $P_B(n, m) \Leftarrow 255$
    else if $s(n, m)$ inside any $Q_l, l = 1, ..., L$ **then**
      $P_B(n, m) \Leftarrow 0$
    else
      if $Pr(obj|i)$ for any $P_k, k = 1, ..., K \neq 0$ and $Pr(obj|i)$ for any $Q_l, l = 1, ..., L \neq 0$ for current background pixels **then**
        $Pr(obj|I) \Leftarrow \frac{d(s,P)^{-1}}{d(s,P)^{-1}+d(s,Q)^{-1}}$
        $Pr(non\_obj|I) \Leftarrow \frac{d(s,Q)^{-1}}{d(s,P)^{-1}+d(s,Q)^{-1}}$
        $Pr(i|non\_obj, I) \Leftarrow \frac{Pr(i|I)-Pr(i|obj,I)Pr(obj|I)}{Pr(non\_obj|I)}$
      else
        $Pr(obj|I) \Leftarrow 0.5$
        $Pr(non\_obj|I) \Leftarrow 0.5$
        $Pr(i|non\_obj, I) \Leftarrow \frac{Pr(i|I)-Pr(i|obj,I)Pr(obj|I)}{Pr(non\_obj|I)}$
      end if
      if $Pr(i|obj, I) \geq Pr(i|non\_obj, I)$ **then**
        $P_B(n, m) \Leftarrow 255$
      else
        $P_B(n, m) \Leftarrow 0$
      end if
    end if
  end for
end for

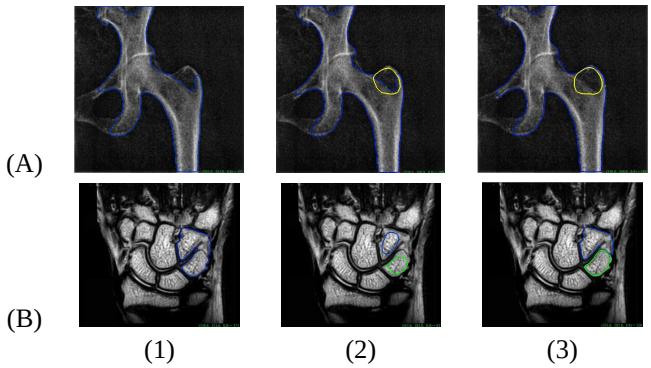

Fig. 4. Segmentation using AVM. (A)The X-ray spine image. (B) The MRI wrist image. (1) Segmentation result without interaction (Spine: $p = 0.98$, $q = 0.98$; Wrist: $p = 0.97$, $q = 0.62$). (2) The initial contour and interactive polygons. (3) Final result (Spine: $p = 0.99$, $q = 0.99$; Wrist: $p = 0.98$, $q = 0.97$).

5. EXPERIMENTS

Fig. 4(A) shows our experiment with only merge polygons for the spine image. Fig. 4(B) shows the experiment with only split polygons for the image. Fig. 5 shows the result with both merge polygon and split polygon for an x-ray leg image. These experiments show that AVM can perform reasonably well for some complicated images with convenient user interaction. We use sensitivity (p) and specificity (q) to measure the accuracy between segmentations with and without interactive polygons.

6. CONCLUSION

In this paper, we introduce a new user interaction method called interactive polygons to help with the segmentation of inhomogenous medical images. The novelty of this interaction method is to integrate region statistics for interactive polygons with the original deformable model. Thus the original deformable model can deform to the desirable boundary despite ambiguity. In our future work, we will also explore adding user scribbles as interaction methods.

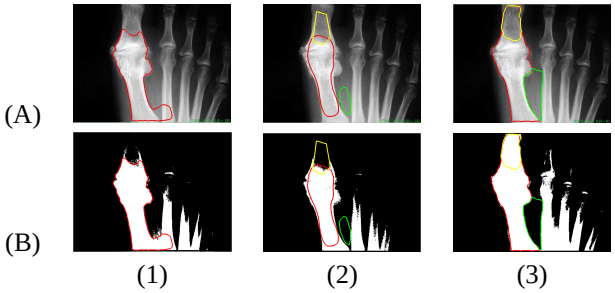

Fig. 5. segmentation using AVM. (A)The x-ray wrist image. (B) The binary ROI image. (1) Segmentation result without interaction ($p = 0.78$, $q = 0.95$). (2) The initial contour and interactive polygons. (3) Final result ($p = 0.97$, $q = 0.99$).

7. REFERENCES

[1] T. Shen, Y. Zhu, X. Huang, J. Huang, D.N. Metaxas, and L. Axel, "Active volume models with probabilistic object boundary prediction module," in *MICCAI (1)*, 2008, pp. 331–341.

[2] M. Kass, A. Witkin, and D. Terzopoulos, "Snakes: Active contour models," *International Journal on Computer Vision*, vol. 1, pp. 321–331, 1987.

[3] P. Fua and C. Brechbühler, "Imposing hard constraints on soft snakes," in *ECCV*, 1996, pp. 495–506.

[4] T. McInerney and D. Terzopoulos, "T-snakes: Topology adaptive snakes," *Medical Image Analysis*, vol. 4, no. 2, pp. 73 – 91, 2000.

[5] L. Grady, "Random walks for image segmentation," *IEEE Transactions on Pattern Analysis and Machine Intelligence*, vol. 28, no. 11, pp. 1768–1783, 2006.

[6] A. Blake, C. Rother, M. Brown, P. Perez, and P. Torr, "Interactive image segmentation using an adaptive GMMRF model," in *ECCV*, 2004, pp. 428–441.

[7] C. Li, C. Kao, J.C.Gore, and Z. Ding, "Minimization of region-scalable fitting energy for image segmentation," *IEEE Trans. Imag. Proc.*, vol. 17, no. 10, pp. 1940–1949, October 2008.